

Electrostatic energy harvesting using capacitive generators without control circuits

Antonio Carlos M. de Queiroz¹

Received: 29 September 2014/Revised: 11 March 2015/Accepted: 13 June 2015/Published online: 23 June 2015
© Springer Science+Business Media New York 2015

Abstract This work discusses and analyzes in detail the operation of some structures of electrostatic generators that can be used for energy harvesting from mechanical vibrations or rotating movement, that do not require any active control circuit for their operation. The structures use an unstable generator based on Bennet's doubler to bias another similar generator, or just to bias one or two variable capacitors, which form the main generator. Their action is similar to electric generators based on electrets, but they are purely based on variable capacitances. Theoretical analyses and experimental results are presented.

Keywords Energy harvesting · Electrostatic generator · Low-power circuits

1 Introduction

In the last years, significant research has been done on the use of microelectromechanical (MEMS) devices for energy harvesting from mechanical vibrations. Very compact electric generators seem to be possible in this technique, using the same technology used in the construction of capacitive accelerometers. It is also possible to exploit the fact that at small distances (tens of μm) greater electric fields are tolerable without sparking than at macroscopic distances, resulting in generators with useful values of energy density (output power per volume) [1]. Most of the

recently proposed generators are based on a single variable capacitor [2], possibly using an electret for biasing [3]. Purely electrostatic generators based on a single variable capacitor were described in many works, usually requiring a DC/DC converter to extract energy from the devices, in some cases with the operation depending on carefully synchronized operation of the converter at certain instants of the vibration cycle. As these small generators do not produce much power, the powering of the control system by the generator is a significant problem. Moreover, most devices also require a battery for startup, taking energy from it and returning it increased after a cycle of operations.

In [4, 5] a different idea was considered, adapting the idea of the “doubler of electricity” or “Bennet's doubler” [6]. This simple electrostatic machine (see Fig. 1) comprises a moveable plate B that forms with two other plates A and C complementary variable capacitors, with contacts between the plates and to ground (by touching the plates) made as shown in the two phases of operation. Plate A is the output terminal, shown as the top plate of an electro-scope. Supposing the plates initially charged with $\pm Q$ in plates A and B , in phase ϕ_1 an inverted copy of $-Q$ in plate B is attracted from ground to plate C . In phase ϕ_2 , this charge is added to the charge in plate A , doubling it, while the charge in plate B is doubled too with $-Q$ coming from the ground. Note that in phase ϕ_2 the potential at plate A is not high, as shown in the electro-scope, because of the high capacitance between plates A and B . It fully appears only at the next phase ϕ_1 . Each repetition of the cycle ideally doubles the charges. An electronic version of the doubler can be built by replacing the connections by diodes, eliminating the need of synchronized switching (Fig. 2(a)), and using two complementary variable capacitors for the plates.

✉ Antonio Carlos M. de Queiroz
acmq@ufrj.br

¹ COPPE/EP – Electrical Engineering Program,
Federal University of Rio de Janeiro,
CP 68504, Rio de Janeiro 21941-972, RJ, Brazil

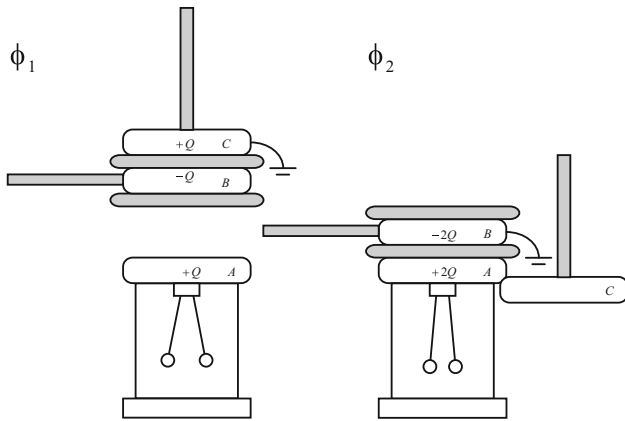


Fig. 1 Bennet's doubler charging an electroscop

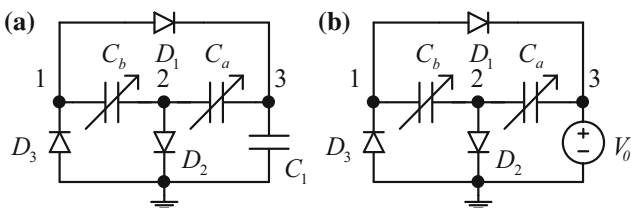


Fig. 2 Electronic doubler charging a capacitor (a) or a battery (b)

A storage capacitor or a battery can be directly charged by the device, without need of a DC/DC converter or any control circuit, as shown in Fig. 2(b). The doubler can also be used by making it charge first a storage capacitor, as in Fig. 2(a), and dumping periodically the accumulated energy to the battery using a DC/DC converter. With a capacitive load, and sufficient capacitance variation (greater than 1.618:1 for complementary variation or greater than 2:1 if C_b is fixed [4, 5]), the device is an unstable circuit, producing an exponentially growing voltage over the storage capacitor C_1 , starting from any small residual or induced charge in the device. The voltages and charges are multiplied by a factor z at each cycle, which can be calculated as function of the capacitances C_a and C_b at the two phases and of C_1 , ignoring losses and other capacitances, as:

$$z = \frac{C_1^2(C_{a1} + C_{b1}) + C_1(C_{a1}C_{a2} + C_{b1}(2C_{a2} + C_{b2})) + C_{a1}C_{b1}(C_{a2} + C_{b2})}{(C_1 + C_{a2} + C_{b2})(C_1(C_{a1} + C_{b1}) + C_{a1}C_{b1})} \quad (1)$$

C_{a1} and C_{b2} are small, and C_{a2} and C_{b1} big, corresponding to the positions of the plates in Fig. 1. This work describes some applications of the doubler where it is used in the production of significant output power at low voltage over a load, without need of active switching or of a control circuit. The studied configurations are not necessarily

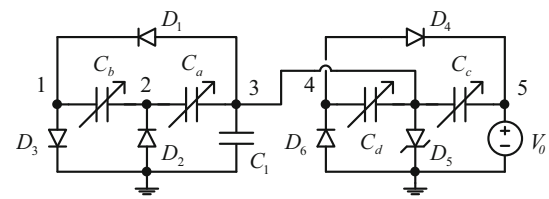


Fig. 3 Directly connected doubler with another doubler for bias

efficient in the energy conversion, and are normally inferior in output power to configurations using energy accumulation in a capacitor with periodical discharges using a DC/DC converter. The absence of a controller, and the economy of the power required by it, however, may turn them competitive. The following sections follow the same organization and materials introduced in [7], with a detailed theoretical analysis of the different situations added.

2 The biased directly connected doubler

The use of bias at the node between the variable capacitors was already mentioned in [5], for the directly connected battery charger and for the doubler with capacitive load. A simple way to generate the required negative bias is to use another doubler with the diodes inverted. This auxiliary device can be smaller than the main device, as its output charge is not consumed, except for leakage. The resulting structure is shown in Fig. 3. An avalanche diode D_5 is used as a shunt regulator to limit the bias voltage (otherwise it may grow until the breakdown voltage of the parts). C_1 is used just to keep the voltage at node 3 approximately constant, and can be omitted without significant differences.

The unstable doubler used for bias quickly charges itself in a few tens of cycles, producing the bias voltage V_b in node 3, the negative of the avalanche voltage of D_5 . Figure 4 shows an example of the waveforms in the biased doubler.

With the voltages at nodes 3 and 5 assumed fixed, C_c has no function, as it takes charge from the battery in the transition to ϕ_2 and returns it in the transition to ϕ_1 . In ϕ_1 the voltage at node 4 is $e_{41} = -V_d$ due to the voltage drop V_d in diode D_6 . The transition to ϕ_2 first goes to point x (see Fig. 5), where $e_{4x} = V_o + V_d$. As the charge in C_d does not change, C_d has the value:

$$C_{dx} = C_{d1} \frac{V_b + V_d}{V_b - V_o - V_d} \quad (2)$$

Completing the transition to ϕ_2 , D_4 conducts and transfers a charge Q_4 to V_o . The voltage over C_d follows the equation:

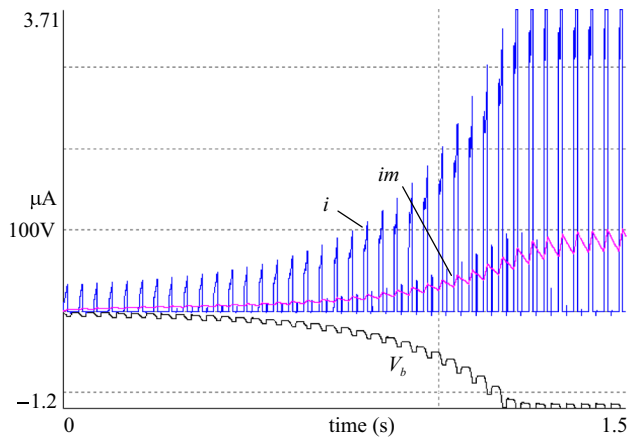


Fig. 4 Simulated startup waveforms for the circuit in Fig. 3, without C_1 . Bias voltage V_b at node 3, current in the battery i , and its average value im

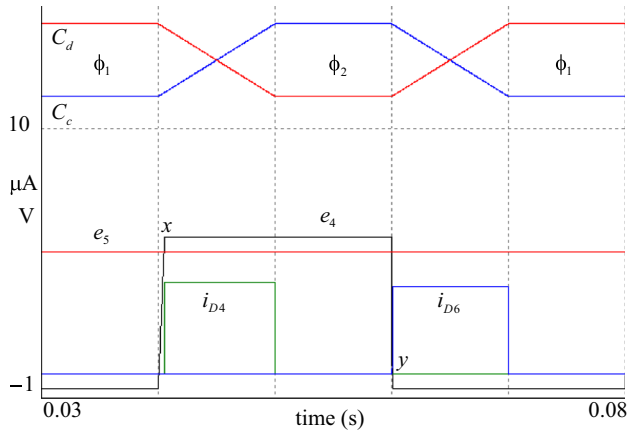


Fig. 5 Ideal waveforms in the biased doubler

$$v_{Cd2} = v_{Cdx} \frac{C_{dx}}{C_{d2}} + \frac{1}{C_{d2}} Q_4 \quad (3)$$

As $v_{Cd2} = v_{Cdx} = V_b - V_d - V_o$, the average current delivered to V_o for operation at a frequency f is:

$$\bar{i}_{D4} = fQ_4 = f(C_{d2}(V_b - V_d - V_o) - C_{d1}(V_b + V_d)) \quad (4)$$

In the next transition to ϕ_1 , the same charge is transferred to C_d through D_6 . For example, consider the doubler used in the experiments in [5], with 10–100 pF capacitance variation, biasing a new device built with 33–330 pF variation. For operation at 25 Hz, $V_o = 5$ V, $V_d = 0.6$ V, and $V_b = -120$ V, the predicted average current is 0.88 μ A. A precise simulation of the circuit in Fig. 3, shown in Fig. 4, even without C_1 to smooth out V_b , results in ~ 0.89 μ A.

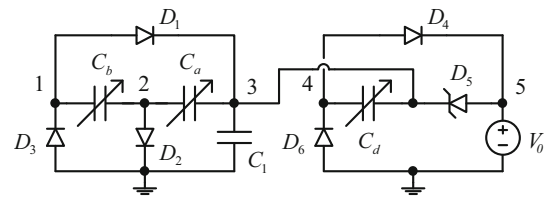


Fig. 6 Variable capacitor biased by a doubler

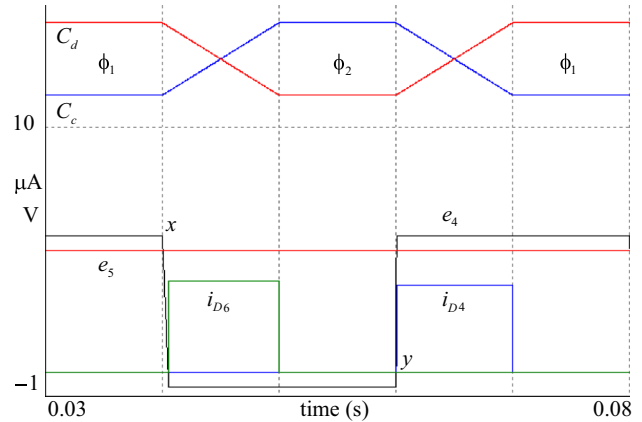


Fig. 7 Ideal waveforms in the biased variable capacitor

3 Biased variable capacitors

The variable capacitor C_c in Fig. 3 can then be eliminated with little difference in the operation. With the second doubler so simplified, the polarity of the bias voltage can be positive, with D_5 inverted. The wasted current through D_5 can be then sent to the output, increasing a bit the charging current. The modified circuit, essentially just a biased variable capacitor generator [8], is shown in Fig. 6.

Assuming C_1 large enough to keep e_3 constant, the waveforms for this case are shown in Fig. 7. The situation is similar to the first case, with the voltage over C_d in the transition from point y to ϕ_1 following the equations:

$$v_{Cd1} = v_{Cdy} \frac{C_{dy}}{C_{d1}} + \frac{1}{C_{d1}} Q_4 \quad (5)$$

$$C_{dy} = C_{d2} \frac{V'_b + V_d}{V'_b - V_o - V_d}$$

As $v_{Cd1} = v_{Cdy} = V'_b - V_d - V_o$ the current through D_4 is calculated as (6), with V'_b being the avalanche voltage of D_5 added to V_o .

$$\bar{i}_{D4} = fQ_4 = f(C_{d1}(V'_b - V_o - V_d) - C_{d2}(V'_b + V_d)) \quad (6)$$

It is the same current (4), since $V'_b = -V_b + V_o$.

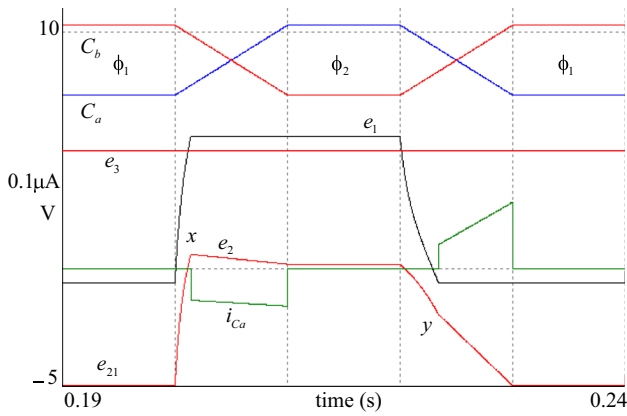


Fig. 8 Ideal waveforms in the biasing doubler with symmetrical capacitance variation. $V'_b = 5$ V

The added current through D_5 is the output current of the biasing doubler feeding a voltage source V'_b . An example of the waveforms for this case is shown in Fig. 8, with V'_b of just 5 V, to allow observation of the effects of the diode drop voltages. At the first ϕ_1 , $e_1 = -V_d$ and e_2 is at a certain negative voltage e_{21} . In the evolution to point x , e_2 grows to the point where D_2 starts to conduct, and $e_{2x} = V_d$. As charges are conserved during the transition:

$$\begin{aligned} C_{a1}(V'_b - e_{21}) &= C_{ax}(V'_b - e_{2x}) \\ C_{b1}(e_{21} + V_d) &= C_{bx}(e_{2x} - V'_b - V_d) \\ C_{bx} &= \frac{(C_{b2} - C_{b1})(C_{a2} - C_{ax})}{C_{a1} - C_{a2}} + C_{b2} \end{aligned} \tag{7}$$

The voltage e_{21} can be calculated from these equations, resulting in a complicated expression. For symmetrical capacitance variation, $C_{b2} = C_{a1}$ and $C_{b1} = C_{a2}$, it reduces to:

$$e_{21} = \frac{C_{a1}V_dV'_b + C_{a2}(V_d^2 - V'_b{}^2)}{C_{a1}V'_b + C_{a2}(V'_b - V_d)} \tag{8}$$

During the final transition to ϕ_2 , a charge Q_1 is transferred to C_a and C_b through D_1 (i_{Ca} in Fig. 8) This same charge is transferred to V'_b after point y . The equations that describe the transition are:

$$\begin{aligned} v_{Ca2} &= v_{Cax} \frac{C_{ax}}{C_{a2}} + \frac{1}{C_{a2}} Q_1 \\ v_{Cb2} &= v_{Cbx} \frac{C_{bx}}{C_{b2}} + \frac{1}{C_{b2}} Q_1 \\ v_{Cax} &= V'_b - e_{2x} = V'_b - V_d; v_{Cbx} = e_{2x} - V'_b - V_d = -V'_b \\ v_{Ca2} &= V'_b - e_{22}; v_{Cb2} = e_{22} - V'_b - V_d \end{aligned} \tag{9}$$

Combining all the equations, the value of Q_1 can be found. The result for symmetrical capacitance variation was shown in [5] (in a different equivalent way). The current delivered to V_o through D_5 is then fQ_1 :

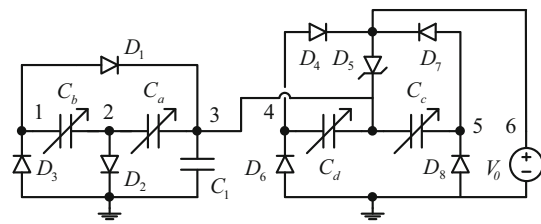


Fig. 9 Double variable capacitor biased by a doubler

$$\bar{i}_{D5} = f \frac{\left((C_{a1}(V_d - V'_b) - C_{a2}V'_b) \right)}{(C_{a1} + C_{a2})(C_{a1}V'_b + C_{a2}(V'_b - V_d))} \tag{10}$$

With 10–100 pF capacitance variation, $f = 25$ Hz too, and $V'_b = 125$ V, a current through D_5 of 0.2523 μ A is predicted. Through the rectifier, the average current, from (6), is 0.88 μ A. The total predicted current is then 1.13 μ A. With the same parameters and $C_1 = 2.2$ nF, a simulation of this structure generates a charging current of ~ 1.1 μ A. The increase due to the current through D_5 is significant. C_1 is necessary. Without it the voltage at node 3 varies significantly, because C_d is much larger than C_a and C_b , and the current drops to 0.54 μ A. Equation (8) predicts $e_{21} = -4.97$ V for $V'_b = 5$ V (Fig. 8) and $e_{21} = -114$ V for $V'_b = 125$ V.

With a double complementary variable capacitor available, the other capacitor can be used too, almost doubling the output current, with the addition of another rectifier, as in Fig. 9. The currents through D_4 and D_7 are as in the previous circuit and the current through D_5 too. A total current of 2.02 μ A is then predicted. A simulation with the same parameters results in this same current. C_1 makes little difference due to the symmetry.

4 Using just two variable capacitors

The doubler can also be built with C_b fixed, at the expense of a smaller voltage multiplication factor per cycle in the startup. The connections of a doubler with two complementary variable capacitors can be modified, with one of the capacitors used in a biasing doubler with fixed C_b , and the other used as a variable capacitor driving a rectifier. This structure is shown in Fig. 10. The value of C_b is not critical. A value somewhat smaller than the maximum C_a seems adequate, resulting in a fast startup of the charging doubler. This structure is equivalent to the one in Fig. 6, but with the variable capacitors of a single symmetrical doubler used, eliminating the need of another smaller doubler for bias generation. With both variable capacitors assumed as identical and large, the current through the

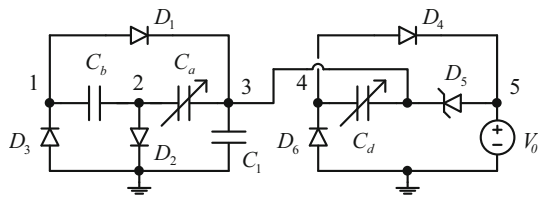


Fig. 10 Doubler with fixed C_b biasing a variable capacitor

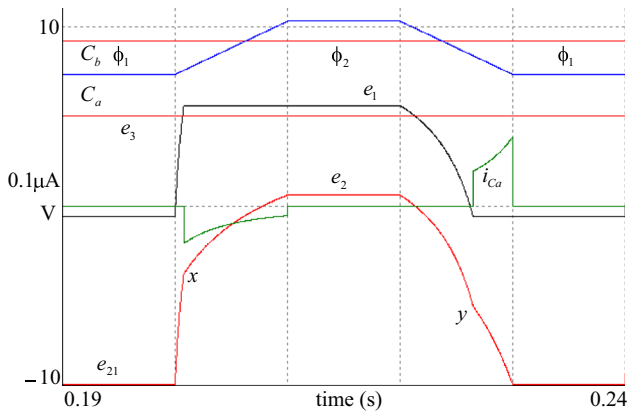


Fig. 11 Ideal waveforms in the biasing doubler with C_b fixed. $V'_b = 5$ V

avalanche diode added to the output current is larger. The analysis of this case differs a bit from the case where the biasing doubler has symmetrical capacitance variation, because e_{2x} is still negative (see Fig. 11, where $V'_b = 5$ V was used too for better visualization), and D_2 is at the edge of conduction after the transition to phase ϕ_2 , where $e_{22} = V_d$. This situation was also cited in [5]. The analysis is simpler than in the previous case because e_{22} is known. Following the mesh from V'_b to D_3 through C_a and C_b at the transition from point y to ϕ_1 , where a charge Q_3 flows:

$$V'_b = v_{Cay} \frac{C_{ay}}{C_{a1}} - \frac{Q_3}{C_{a1}} + v_{Cby} - \frac{Q_3}{C_b} - V_d$$

$$v_{Cay} = V'_b - e_{2y} = (V'_b - V_d) \frac{C_{a2}}{C_{ay}}; v_{Cby} = e_{2y} + V_d = -V'_b$$

(11)

Q_3 can be immediately obtained from these equations, and the charging current through D_5 is calculated as:

$$\bar{i}_{D5} = fQ_3 = f \frac{V'_b \left(\frac{C_{a2}}{C_{a1}} - 2 \right) - V_d \left(1 + \frac{C_{a2}}{C_{a1}} \right)}{\frac{1}{C_{a1}} + \frac{1}{C_b}}$$

(12)

Just to complete the analysis, the voltage e_{21} can be calculated for this case too by observing that in the transition between point y and ϕ_1 :

$$v_{Cb1} = e_{21} + V_d = v_{Cby} - \frac{Q_3}{C_b}$$

(13)

Using (13) and (11), e_{21} is found as (14):

$$e_{21} = \frac{C_{a1}V'_b + C_{a2}(V_d - V'_b) - C_b(V_d + V'_b)}{C_{a1} + C_b}$$

(14)

With 33–330 pF variable capacitors and $C_b = 220$ pF, (6) and (12) add to $0.88 \mu\text{A} + 0.71 \mu\text{A} = 1.6 \mu\text{A}$. A simulation with the, required, $C_1 = 2.2$ nF, results in about this same value. Equation (14) predicts $e_{21} = -9.96$ V for $V'_b = 5$ V (Fig. 11) and $e_{21} = -255$ V for $V'_b = 125$ V. The energy conversion is inefficient due to the relatively large power wasted in D_5 . Note that both currents, through C_a and through D_5 , are always similar when the biasing doubler and the variable capacitor generator use the same variable capacitances. A more rational implementation of this generator could use C_a smaller than C_d .

5 Experimental evaluation

All the structures were tested using as bias generator the rotating doubler used in [5], implementing two complementary variable capacitors varying between 10 and 100 pF with one cycle per turn, and a new doubler with capacitance variation of 33–330 pF with two cycles per turn, shown in Fig. 12.

The device has four sets of six $\sim 7 \times 7$ cm fixed plates interconnected diagonally that form two complementary variable capacitors with five double plates in the rotor, with maximum capacitances at both diagonal positions of the rotor. The diodes are of the type used in microwave ovens, which have very low leakage and capacitance, and can safely operate up to the ~ 3.5 kV that the device can reach before sparking between the plates occurs. Their voltage



Fig. 12 New experimental doubler

drop is high, ~ 5 V, but the doubler works perfectly well with them. A DC motor can turn it at a few tens of cycles per second. The proposed structures were tested with the battery replaced by a $1\text{ M}\Omega$ resistor ($909.1\text{ k}\Omega$ of load counting the $10\text{ M}\Omega$ oscilloscope probe) in parallel with a 100 nF capacitor, to simplify the measurement of the output current. With this load, the obtained output voltage is smaller than the 5 V assumed before, but the difference in the generated current is small due to the much larger bias voltages (with a 120 V avalanche diode). The measurements in the following subsections were compared with simulations of the same structures and with the deduced formulas with good agreement.

5.1 Biased doubler

The $33\text{--}330\text{ pF}$ doubler was operated at 12.5 turns/second, resulting in 25 cycles/second. The biasing doubler was operated at a smaller speed (about 10 Hz) and not synchronized with the other. Figure 13 shows the measured output voltage, with average value of 0.7 V , corresponding to $0.77\text{ }\mu\text{A}$. An ideal simulation, which agrees with (4), gives a slightly larger voltage, 0.79 V . There is some uncertainty in the variable capacitance limits, and the avalanche diode probably conducts significantly somewhat before the nominal avalanche voltage in this very low current application. There is also the effect of stray capacitances and leakage, not considered in the analyses. Similar concordances were obtained for the other structures. Figure 14 shows the startup of the system, with the similarity to the ideal waveform in Fig. 4 observable. The startup is slower than in Fig. 4 because the biasing doubler was running more slowly.

To test the capability of the experimental setup, D_5 was removed and the speed doubled. The bias voltage climbed to about 2.3 kV , limited only by sparking, and the output

voltage reached more than 30 V , at $33\text{ }\mu\text{A}$, corresponding to about 1 mW of output power.

5.2 Biased variable capacitor

With the circuit in Fig. 6, some extra current is obtained with the current through D_5 sent to the output. The bias voltage is also slightly increased. Figure 15 shows the output voltage with average value of 0.8 V , with $0.88\text{ }\mu\text{A}$. The irregular appearance is due to the operation of the biasing doubler not synchronized with the operation of the variable capacitor. Without the current through D_5 , the voltage drops to 0.62 V . The circuit with two complete doublers produces slightly greater current in this case, due to the more uniform loading of the biasing doubler.

5.3 Biased double variable capacitor

Using both capacitors of the second doubler as variable capacitors driving rectifiers, as in Fig. 9, the result is shown

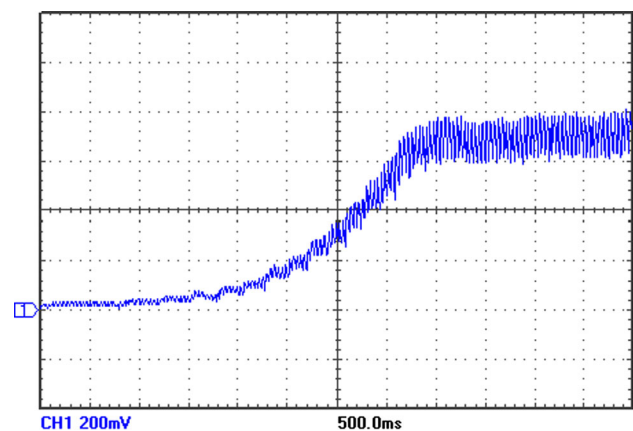


Fig. 14 Startup of the biased doubler

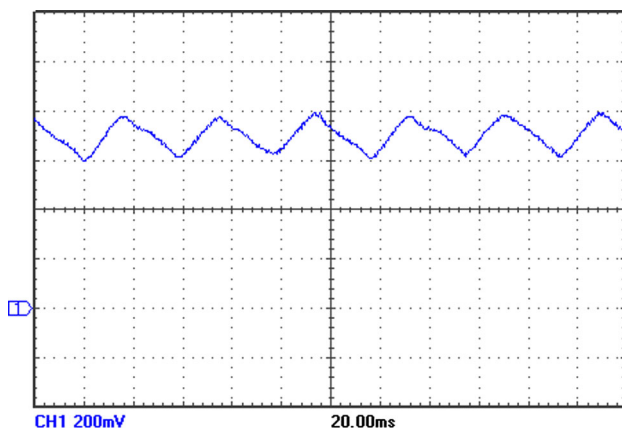


Fig. 13 Output voltage of the biased doubler

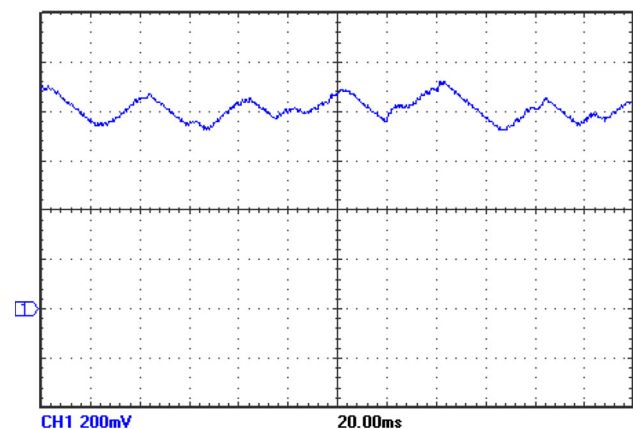


Fig. 15 Output voltage of the biased variable capacitor circuit

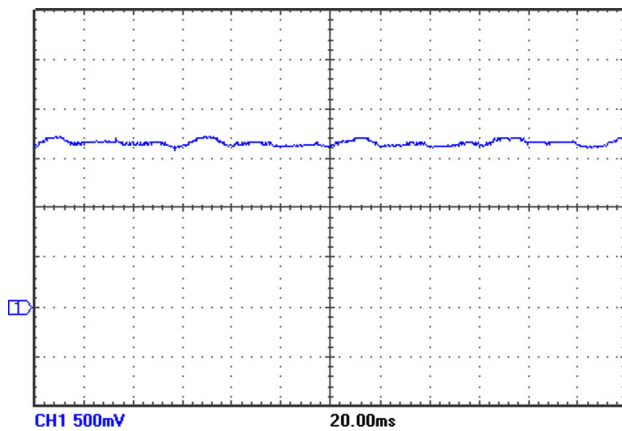


Fig. 16 Output voltage of the double biased variable capacitor circuit

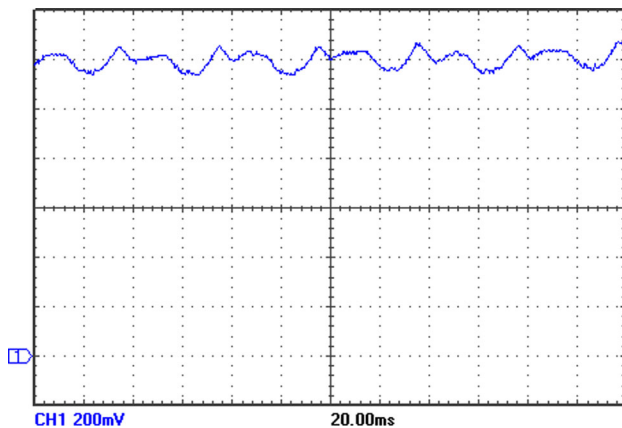


Fig. 17 Output voltage of the circuit with two variable capacitors

in Fig. 16. The output voltage is more than doubled in relation to the single variable capacitor version, reaching 1.7 V at 1.9 μA . Without the current through D_5 , the output voltage drops to 1.5 V. Again, the irregular voltage is due to not synchronized operation of the two devices. It can be observed that the variable capacitors charge the output at each 20 ms, while D_5 charges at each ~ 60 ms.

5.4 Two variable capacitors

The circuit in Fig. 10 results in the output shown in Fig. 17. The synchronized operation of the biasing doubler and of the biased variable capacitor at 25 Hz can be observed. The variable capacitor generates 0.7 μA , and the current through D_5 another 0.6 μA , that add to create the observed 1.2 V, 1.3 μA at the load.

6 Conclusions

The possibility of using the unstable circuit of the electronic electrostatic doubler as bias generator for another doubler or just for variable capacitors was studied in detail and experimentally demonstrated. In all cases tried the biasing doublers did not require any explicit initial charge, starting from electrical noise or external electrical interference (unavoidable in the experimental setup used, with the extremely high impedance of the circuits), eliminating the need of batteries or other devices for precharging. The capacitive generators are highly efficient, with important losses only in the shunt regulator that limits the bias voltage. Part of the wasted energy can be used by routing the regulator current to the output, with significant effect in the experimental realizations, because a relatively large biasing doubler was used. All the structures are compatible with MEMS fabrication, taking power only from mechanical vibrations. It remains to be verified, however, if the obtainable insulation is high enough for the unstable operation of the doubler, and if reliable startup of the doubler can be obtained with small structures without some explicit charge source for startup. In any way, if a startup source is required, it is not critical, as once started the doubler easily reaches any required biasing voltage without further external input. The developed analysis of the structures was shown to be realistic enough to predict the behavior of the devices with good accuracy.

References

- Torres, J.-M., & Dhariwal, R. S. (1999). Electric field breakdown at micrometre separations. *Nanotechnology*, *10*(1), 102–107.
- Yen, B., & Lang, J. (2006). A variable-capacitance vibration-to-electric energy harvester. *IEEE Transactions on Circuits and Systems I*, *53*(2), 288–295.
- Edamoto, M., Suzuki, Y., Kasagi, N., Kashiwagi, K., Morizawa, Y., Yokoyama, T., et al. (2009). Low-resonant-frequency micro electret generator for energy harvesting application. *IEEE 22nd International Conference on Microelectromechanical Systems* (pp. 1059–1062). Sorrento, Italy.
- de Queiroz, A. C. M. (2010). Electrostatic vibrational energy harvesting using a variation of Bennet's doubler. *2010 53rd IEEE Midwest Symposium on Circuits and Systems* (pp. 404–407). Seattle, USA.
- de Queiroz, A. C. M., & Domingues, M. (2011). The doubler of electricity used as a battery charger. *IEEE Transactions on Circuits and Systems II*, *58*(12), 787–801.
- Bennet, A. (1787). An account of a doubler of electricity. *Philosophical Transactions of the Royal Society of London*, *77*(2), 288–296.
- de Queiroz, A. C. M. (2014). Electrostatic energy harvesting without active control circuits. *2014 IEEE Latin American Symposium on Circuits and Systems* (pp. 1–4). Santiago, Chile.
- Le May, D. B., Drexel, C. (1963). Electrostatic generator. *U. S. patent 3094653*.



Antonio Carlos M. de Queiroz received the B. Sc. EE. Degree in 1979, the M. Sc. EE. Degree in 1984, and the D. Sc. EE. Degree in 1990 from the Universidade Federal do Rio de Janeiro, Rio de Janeiro, Brazil. Since 1982 he has been with the same institution, where he is now Titular Professor at the Department of Electronic Engineering and at the Electrical Engineering Program of the Coordenação dos Programas de Pós-graduação em Engenharia

(COPPE). His main interests are in general circuit theory, filters and

signal processing, computer-aided synthesis and analysis of circuits, energy harvesting using electrostatic generators, and the history of electricity.